J Mar Sci Technol (2004) 9:171–181
DOI 10.1007/s00773-004-0181-y

Journal of
Marine Science
and Technology

Axial vibrations of a propulsion system taking into account the couplings and the boundary conditions

Lech Murawski

Centrum Techniki Okrętowej (Ship Design and Research Center), S.A., ul. Waky Piastowskie 1, 80-958 Gdainsk, Poland

Abstract Calculations of the axial vibrations of a marine power transmission system are a very difficult problem owing to the complicated couplings and difficulties in determining the boundary conditions. The torsional–bending–axial coupling action of the system should be accounted for when considering its dynamics. A determination of the mutual interference of system vibrations and their boundary conditions is also necessary. A performance analysis of the main engine bearings, the thrust bearings, and the axial dampers should also be carried out. Thus, the effects of additional bending stresses in the crankshaft and possible vibrations of the ship's structure due to the reaction force in the thrust bearings should be considered. I have devised a computer program to analyse the axial vibration problem. The numerical analysis method presented is compared with measurements (performed on real ships) and verified by them.

Key words Longitudinal vibration · Axial vibration · Propulsion system · Thrust bearing · Axial damper · Engine main bearing · Oil film stiffness and damping · Crankshaft–propeller phasing

1 Introduction

Axial (longitudinal) vibrations are the result of the pulsing hydrodynamic forces induced on the propeller and dynamic longitudinal deformations of the crankshaft.[1] When a crank throw is loaded by gas pressure and mass forces through a connecting rod mechanism, the arms of the crank throw deflect in the axial direction of the crankshaft, exciting axial vibrations. These vibrations may cause the engine crankshaft to fail with increasing frequency. The propulsion system is connected to the ship's hull through a thrust bearing. Therefore, the axial vibrations are transferred to different regions of the ship's hull structure through a thrust bearing (and possibly an axial damper) and the ship's double bottom.[2] Excessive superstructure vibrations worsen the working conditions of the ship's crew and may influence maritime safety detrimentally.

Generally, axial vibrations are only dangerous for propulsion systems with slow-speed, two-stroke engines and propellers directly driven by shaft lines.[3] Nowadays, all slow-speed engines are equipped with an axial damper. If the damper is well regulated, axial vibrations are no danger to the main engine. Nevertheless, these vibrations have to be controlled by checking (by calculations and/or measurements) the vibration amplitude of the free end of the crankshaft. Numerical analyses should determine the operating restrictions for a main engine with a failed axial damper. Usually the maximal rotational speed of the engine is limited.

A determination of the coupling degree of the axial vibration with other vibrations, crankshaft deformation analysis, and torsional vibration calculations are necessary in order to get an appropriate determination of the axial vibrations. An appropriate determination of the dynamic characteristics of the engine's main bearings and thrust bearings, and of the axial dampers of the propulsion system may be crucial for a suitable estimation of the axial vibrations.

However, it is not only the dynamic behavior of the propulsion system which should be analyzed during ship design. Calculations of the ship's hull and superstructure vibrations are nearly as important as dynamic analyses of the power transmission system.[4] These are not separate problems. The thrust bearing and axial damper reactions (coming from the vibrations of the longitudinal propulsion system) are one of the ship's hull and deckhouse excitation forces. Therefore, these dynamic reactions should also be determined.

I created a computer algorithm to analyse the longitudinal vibration problem. Nonlinear algorithms to determine the dynamic stiffness and damping characteristics

Address correspondence to: L. Murawski (lmur@cto.gda.pl)
Received: September 22, 2003 / Accepted: May 11, 2004

of the thrust bearing, the engine main bearing, and the axial damper are proposed here. A crankshaft deformation analysis to determine the torsional–bending–longitudinal vibration coupling coefficients was also carried out. A crankshaft–propeller phasing analytical method is proposed in this article. All numerical algorithms were verified by measurements.

2 The computational method

The mathematical model of a marine power transmission system designed for axial vibrations analysis is usually isolated from the ship's hull. In general, specialized software is based on the finite-element method (FEM). Typical, 2-node beam elements are used for modeling the propulsion system. There are no geometrical or gyroscopic effects. This assumption is acceptable owing to the low rotational speed of the shaftline (below 180 r.p.m.) and low initial loading.[5] The characteristic matrices (masses, dampings, and stiffnesses) are related to a rotational and axial degree of freedom. Determining the excitation forces (derived from the couplings effects) is the most specific and difficult problem. The main sources of excitations causing axial vibrations can be classified as follows[5,6]:

— crankshaft deformations due to radial gas and inertia forces which are applied to particular cranks (Fig. 1);
— crankshaft deformations due to torsional vibrations of the propulsion system;
— propeller-induced hydrodynamic couplings between torsional and longitudinal vibrations;
— the propeller's direct, longitudinal hydrodynamic forces.

The FEM computer program developed contains the calculation algorithm for the axial vibrations in which all previously mentioned coupling effects are accounted for. In the algorithm, a torsional vibration calculation is performed as the first step in order to take torsional–longitudinal coupling effects into account.

An example of a bending–longitudinal coupling on the 4th crank of a MAN B&W 8 S70 MC-C type engine are shown in Fig. 1 (the coupling coefficients were determined by the Nastran commercial program).

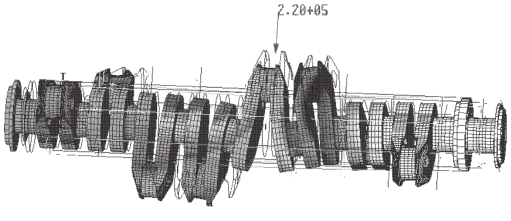

Fig. 1. Bending–longitudinal coupling on the 4th crank of the 8 S70 MC-C engine

The following elements (which are important from a coupled axial vibration analysis point of view) can be distinguished in a real ship's power transmission system: a crankshaft, a shaftline, a screw propeller, couplings, a thrust bearing, the main engine bearings, a torsional vibration damper, and an axial damper. Their stiffness, inertia, and damping values may differ by several orders of magnitude. The dynamic characteristics of some elements (e.g., dampers and bearings) also change with engine speed, and with the loading or longitudinal vibration amplitude. In the calculation algorithm, each element of the motion equation matrices is formed separately. Two determination methods are employed for the characteristic matrix elements. After the first magnitude has been determined, the rest are found on the basis of the producer's technical specifications or empirical relations from available literature. In cases where reliable data were lacking (especially for boundary conditions data), my calculation algorithms were extended. These methods were used to determine the stiffness and damping of the main engine bearings, the thrust bearing, and the axial damper.

The most important value to find was the added water mass of the propeller. There are several formulas describing this value. Quite a good estimation of the added water mass (as well as the damping value) for an axial vibration may be obtained from the Dien and Schwanecke formula.[7] A more complicated formula has been derived on the basis of Parson's theory.

The relative torsional deformation of the crankshaft cranks causes its axial deformation. Similarly, the radial forces cause an axial deformation of the crankshaft.[5] Crankshaft deformation calculations are aimed at determining the ratio (coupling coefficient) of the radial force (and relative torsional amplitude) and the axial force, with the assumption that the axial deformations of the crankshaft due to both loadings is the same. This makes the determination of equivalent axial forces, i.e., shaftline axial vibration excitations, possible. The crankshaft seating boundary conditions, i.e., the dynamic stiffness characteristics of the main engine bearings, should be determined in advance.

3 Coupled excitations

Two types of couplings can be applied to a crankshaft. The first appears if an excitation force in one direction is the cause of vibrations in a perpendicular direction. This type of coupling can be applied if the detuning between the natural frequencies of an analyzed structure is good in both directions, i.e., above 100%. The excitation can then be treated as a quasi-static force. If

the detuning is not good, the coupling coefficient has to be defined as a quotient of the vibration amplitude in one direction and the equivalent excitation force in the perpendicular direction. In my experience, bending–longitudinal couplings through the crankshaft may be treated as the first type, i.e., a force-to-force coupling. The crankshaft's torsional–longitudinal coupling has to be determined as the second type, i.e., an amplitude-to-force coupling. For example, the first natural vibrations of the Sulzer 8 RTA96 C-type crankshaft in the longitudinal, the torsional, and the bending direction are approximately equal to 7.34 Hz, 10.40 Hz, and 36.50 Hz, respectively. Therefore, the bending–longitudinal vibration detuning is very good, while the torsional–longitudinal detuning is poor.

The objective of crankshaft deformation analysis is to determine the ratio of the radial force (or the relative torsional amplitude) to the equivalent longitudinal force, assuming that the axial deformations caused by these loads are the same. This facilitates the determination of the equivalent longitudinal forces (with known radial forces or torsional amplitudes) i.e., the uncoupled longitudinal excitations. The bending–longitudinal coefficient, which reflects the coupling effect of the radial forces and the axial equivalent forces, was defined as:

$$k_{\mathrm{r}} = \frac{F_{\mathrm{R}}}{F_{\mathrm{L}}} \tag{1}$$

where F_{R} is the gas and mass cylindrical radial force, and F_{L} is the equivalent longitudinal force.

An analytical determination of the bending–longitudinal coupling coefficient can be performed by multivariant FEM static, nonlinear calculations. The nonlinearities include the boundary conditions modeling the main engine bearings. The method of determining the stiffness characteristics of the oil film on the bearings is given in Sect. 4.1. Crankshaft deformation calculations should be performed under a longitudinal force and radial forces acting on each crank. The value of the longitudinal force should be assumed in such a way that the deformation of the free end of the crankshaft should be close to a typical axial vibration amplitude for a given engine type (from producer data). The radial forces should be equal to the maximum gas and mass cylindrical forces. An example of the longitudinal loading of the MAN B&W 8 S70 MC-C-type engine is shown in Fig. 2. The crankshaft deformation under radial forces was shown in Fig. 1.

As a result of "longitudinal" calculations, the crank's longitudinal stiffness can be determined according to Eq. 2.

$$k_{\mathrm{l}} = \frac{F_{\mathrm{L}}}{\Delta L} \tag{2}$$

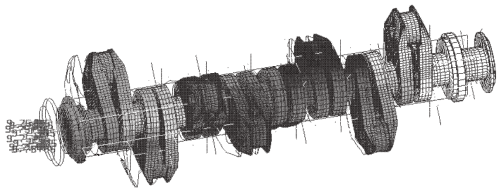

Fig. 2. The 8 S70 MC-C crankshaft deformations under longitudinal loading

where F_{L} is the longitudinal force, and ΔL is the longitudinal deformation of a separate crank.

As a result of "radial" calculations, the coupled bending stiffness of the crank can be determined according to Eq. 3.

$$k_{\mathrm{b}} = \frac{F_{\mathrm{R}}}{\Delta L} \tag{3}$$

where F_{R} is the radial force.

After simple transformations of Eqs. 1–3, the bending–longitudinal coupling coefficients can be determined by Eq. 4 for each crank throw.

$$k_{\mathrm{r}} = \frac{k_{\mathrm{b}}}{k_{\mathrm{l}}} \tag{4}$$

An analytical determination of the torsional–longitudinal coupling coefficient can be performed using methods similar to those used for the bending–longitudinal coefficient. One more variant of the crankshaft deformation calculation has to be performed, i.e., loading by a torque moment. The value of the torque moment should be assumed in such a way that the maximum angular deformation of the crankshaft would be close to the maximal torsional amplitude. The torsional–longitudinal coefficient, which reflects the coupling effect of the torsional deformation of the crankshaft and the equivalent axial forces, was defined as

$$k_{\mathrm{t}} = \frac{\Delta\varphi}{F_{\mathrm{L}}} \tag{5}$$

where $\Delta\varphi$ is the torsional deformation of a separate crank.

As a result of the "torque" calculations, the coupled torsional deformations of the cranks can be determined according to Eq. 6.

$$k_{\mathrm{c}} = \frac{\Delta L}{\Delta\varphi} \tag{6}$$

After simple transformations of Eqs. 2, 5, and 6, the torsional–longitudinal coupling coefficients can be determined by Eq. 7 for each crank throw.

Table 1. Torsional–longitudinal coupling coefficients (deg/*N*) × 10^{-6}

	Cylinder No.							
ME type	1	2	3	4	5	6	7	8
6 RTA58 T-B	0.5737	0.3038	15.01	6.231	0.2949	0.8569		
7 S70 MC-C	0.577	0.404	–1.15	–0.447	–1.58	0.521	1.25	
8 S70 MC-C	0.6121	0.3206	–5.333	–0.2953	–0.3036	–38.08	0.2910	2.055
8 RTA96 C	0.2901	0.1444	139.5	0.1279	0.1299	2.364	0.1364	0.7078

ME, main engine

Table 2. Bending–longitudinal coupling coefficients (*N*/*N*)

	Cylinder No.							
ME type	1	2	3	4	5	6	7	8
6 RTA58 T-B	4.952	5.679	4.223	4.271	5.759	4.867		
7 S70 MC-C	4.951	5.982	5.101	3.142	5.798	6.520	5.909	
8 S70 MC-C	5.760	6.415	4.349	4.207	4.250	4.347	6.218	6.694
8 RTA96 C	3.360	3.683	2.467	1.832	1.842	2.457	3.601	3.728

$$k_t = \frac{1}{k_l \cdot k_c} \tag{7}$$

It should be stressed that according to Eqs. 1 and 5, a decrease in the coupling coefficients leads to an increase in the axial vibration excitations. Several main marine engines were analyzed. Examples of the torsional–longitudinal and bending–longitudinal coupling coefficients are given in Tables 1 and 2, respectively. It is assumed that cylinder 1 is placed in the driving end side of the crankshaft.

The torsional–longitudinal coupling coefficient of a propeller is defined in a similar way to the coefficient of a crankshaft. Determining the coefficient by calculations is much more difficult owing to the 3-D hydrodynamic problem. This coefficient can be determined experimentally by measuring axial vibrations near the thrust bearing. The coefficient determined may be used for calculations on sister ships. Other coupling coefficients can also be estimated by measurements. These measurements should be performed on the free end of the crankshaft as well as at a wide range of main engine speeds, owing to the necessity of separating all types of coupling.

After determining the whole range of coupling coefficients, the values of the engine's radial forces, torsional vibration amplitudes, and the uncoupled, axial, propeller hydrodynamic forces have to be determined. All these forces are specified by the main engine producers and are determined during the design of the propeller.

Torsional vibrations analysis is performed by well-known methods and typical FEM procedures. Torsional amplitudes are calculated for each crank. Coupling coefficients (k_t) are determined by a deformation analysis of the crankshaft. After these calculations, Eq. 5 is used for determining equivalent longitudinal excitations (located on each crank). The equivalent axial forces of the propeller are determined in a similar way.

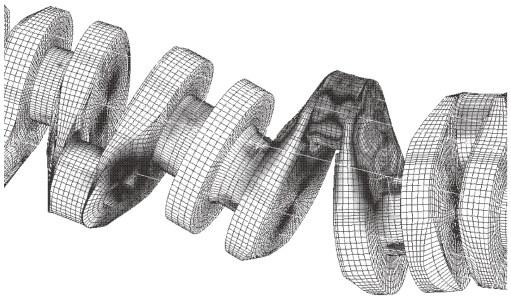

Fig. 3. The 8 RTA96 C crankshaft stress field loaded by a radial force acting on the 4th crank

The mass and gas cylindrical forces are the source of the crank's radial forces. Calculation methods for the radial forces are published by the main engine producers. Coupling coefficients (k_r) are determined by crankshaft deformation analysis. After these calculations, Eq. 1 is used for determining equivalent longitudinal excitations (located on each crank).

The calculations presented above can also be designed for crankshaft strength analysis. An example of the Von-Misses stress field on a crankshaft loaded by a radial force acting on the 4th crank is shown in Fig. 3. The crankshaft of the 8 RTA96 C-type engine presented here is atypical: it is made up of two four-cylinder crankshafts connected by a stiff coupling. This crankshaft is one of the biggest applied in world ship-

building. The crankshaft FEM model is made up of 644 844 degrees of freedom, 215 780 nodes, and 184 828 3-D (8-node) elements.

4 Boundary conditions

The general assumption that the mathematical model of the power transmission system is isolated from the ship's hull makes the boundary conditions important.[8] The quality of the calculations may determine the accuracy of the axial vibration analyses. In the case of the axial vibration calculations, the stiffness and damping characteristics of the thrust bearing and axial damper are the boundary conditions (this refers to propulsion systems with a driven directly propeller by a two-stroke, slow-speed main engine, for which these vibrations can be significant).

During crankshaft deformation analysis (for determining the coupling coefficients, see Sect. 3), a proper determination of the displacement of the crankshaft journals in the main bearings is essential. Therefore, calculations of the stiffness characteristics of the engines main bearings should be carried out.

The calculation algorithms of the bearings and the damper are given in Sects. 4.1–4.3. Generally, the programs are based on the finite difference method. The stiffness and damping characteristics of a typical marine construction are also presented, and the characteristic influences on axial vibrations are analyzed.

4.1 Engine main bearings

The influence of crankshaft displacement in the main bearings on the longitudinal stiffness of the shaft as well as on the values of the torsional–longitudinal and bending–longitudinal coupling coefficients was analyzed. It should be noted that the crankshaft foundation analysis must take into account the dynamic stiffness of the oil film on the bearings and the stiffness of the engine body mounted on the ship's double bottom.

The algorithm of the stiffness of the oil film on the journal bearings and its damping characteristics is based on the finite difference method, which is applied to the Reynolds principle and the Stefan's principle.[9] The main bearings are narrow and their loadings are symmetrical in the longitudinal direction, in contrast to the stern tube bearing. Therefore, the relative deformation of the main bearing journal and tube may be omitted, and the bearings can be modelled as a point-wise support. The main bearings of the engine are intensively loaded and the shaft journal displacements are highly nonlinear. The crankshaft seating should be modelled in such a way that while analyzing crankshaft kinematic deformations, a displacement of the journal at the real

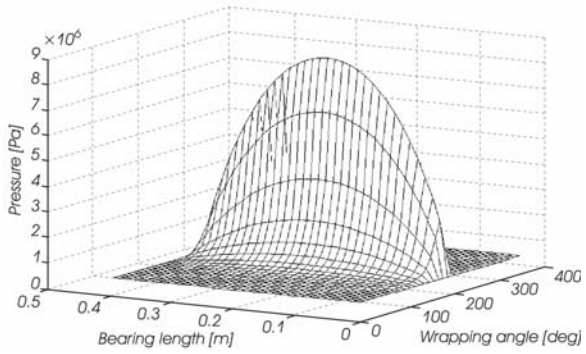

Fig. 4. Pressure distribution of the lubricating oil of the ME (main engine) bearing

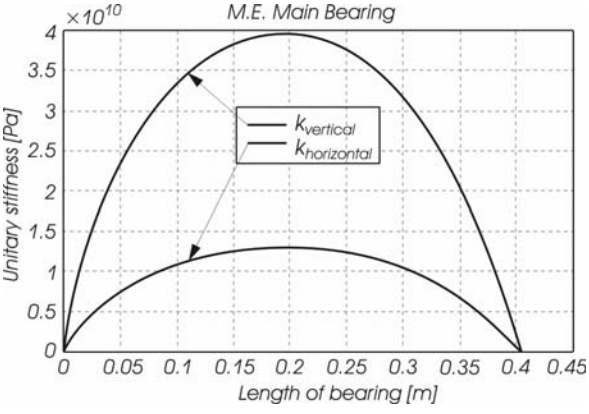

Fig. 5. Dynamic stiffness characteristics of the ME bearing

load of the main bearing is obtained. Typical crankshaft deflections of a slow-speed marine engine are equal to 0.5–0.8 mm.

An example of this calculation was performed for the main bearing of the 8 RTA96 C-type engine installed on a 4400 TEU container ship. The calculated minimum oil film thickness was equal to 45 μm at a nominal engine speed and 36 μm at 50 r.p.m. The lubricating oil film pressure distribution at a nominal engine speed is shown in Fig. 4. The vertical and horizontal (in the crank-related coordinate system) stiffness distribution of the lube oil film along the main bearing is shown in Fig. 5. The absolute values of the oil film stiffnesses of the main bearings and the dampings are as follows: vertical (radial forces direction) stiffness 1.129×10^{10} N/m; horizontal stiffness 5.532×10^{9} N/m; vertical damping 6.934×10^{8} Ns/m; horizontal damping 6.937×10^{8} Ns/m. The stiffness in the loading direction is much higher than that in the perpendicular direction.

The influences of the crankshaft displacement in the main bearings on the crankshaft axial and torsional stiffnesses and on the values of the torsional–longitudinal and the bending–longitudinal coupling coefficients were analyzed. The dislocations of the crankshaft's

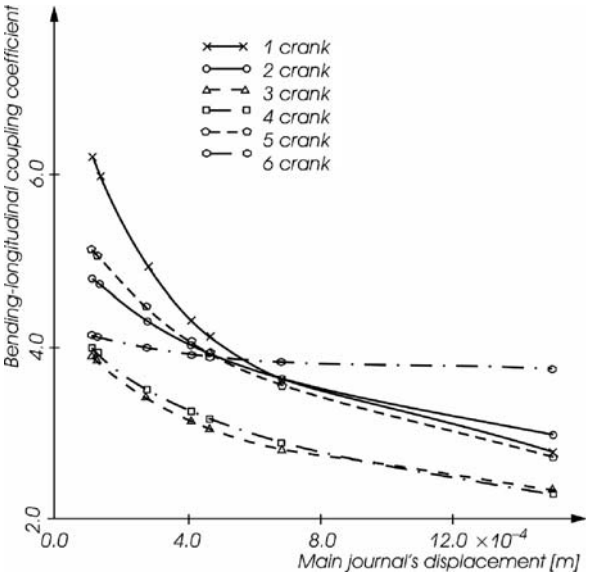

Fig. 6. Bending–longitudinal coupling coefficients versus crankshaft displacement

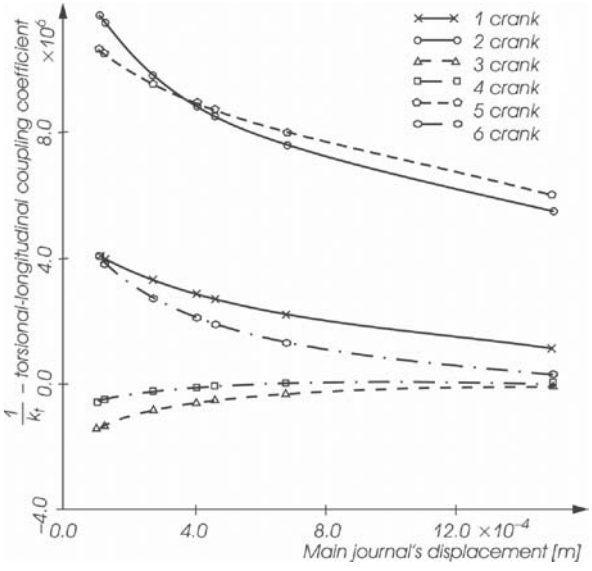

Fig. 7. Torsional–longitudinal coupling coefficients versus crankshaft displacement

main journals account for the dynamic stiffness of the lubricating oil film and the stiffness of the engine frame with its foundations on the ship's double bottom. The influences calculated for the 6 RTA-76-type engine are shown in Figs. 6 and 7. The real crankshaft deflection value in the main bearings of the 6 RTA-76 engine is equal to 0.65 mm.

As is shown in Figs. 6 and 7, the correct estimation of the dislocations of the crankshaft's main journals has a significant influence on the crankshaft stiffnesses and the coupling coefficients. Generally, if the crankshaft foundation flexibility is increased, then the propulsion axial vibrations are more dangerous (the longitudinal stiffness and the bending–longitudinal coupling coefficients of the crankshaft are smaller). Only the axial vibration amplitudes in a torsional vibration resonance might be smaller because of a greater torsional–longitudinal coupling coefficient.

4.2 Thrust bearings

A ship's thrust bearings are subjected to hydrodynamic forces (mainly thrust) generated by the propeller. The static load on the bearing is due to the constant component of these forces. However, the bearings are also subjected to a dynamic load due to the longitudinal vibration of the power transmission system. The marine thrust bearings are those of the Michell type. They are made up of several blocks (segments) supported on an edge, and they are self-aligning. The blocks are placed along the circumference of the thrust flange, but they do not the whole circuit. Only about 70% of the thrust flange surface is supported. The need for the proper loading of the thrust bearing is the reason for this type of construction (the thrust area is determined by the shaft diameter, and is quite big). Consequently, the resultant thrust force axis is not the same as shaft line axis: the acting point of the resultant thrust is situated below the shaft line axis. Therefore, as well as the thrust force, a moment is generated at the shaft and bearing foundation.

The producers of the main engine propose a model for the thrust bearings, which is a single, linear spring. They give a spring stiffness value for each engine type. For most typical marine propulsion systems, this model is sufficient, but for some phenomena and some analytical problems it might be too simple. The producers' model does not take into account the damping property of the oil film and the stiffness of the foundation in a double bottom. If axial vibrations are high in the thrust block area (e.g., for a long shaft line), the nonlinearity of the oil film's characteristics should be taken into account. The dangerous phenomenon of a scarcity of lube oil cannot be analyzed with the producers' simple model.

Specialized software for analyzing the stiffness of a thrust-bearing lube oil film and its damping characteristics has been proposed. In the algorithm, the partial differential Reynolds equation describing the distribution of oil pressure on the thrust-bearing pad has been solved using the finite difference approximation. Marine thrust bearings are constructed with two rows of pads. One row is designed for the ship running ahead, and the second for running astern. On the second row of pads, an additional dynamic force is induced by squeezing out lube oil. This thrust component is significant

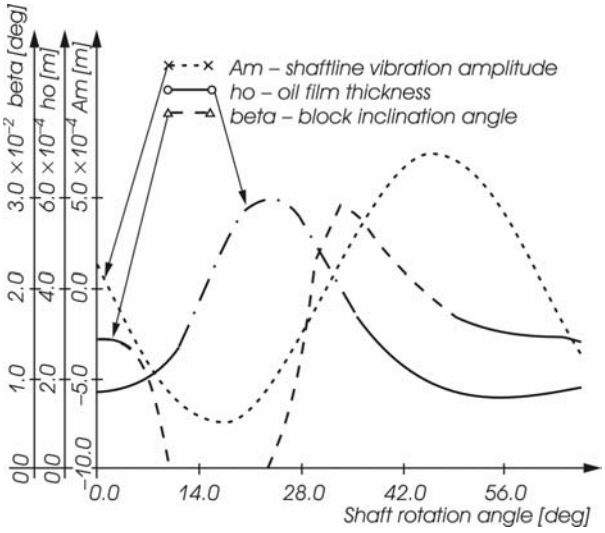

Fig. 8. The bearing operation parameters at 51.2 r.p.m.

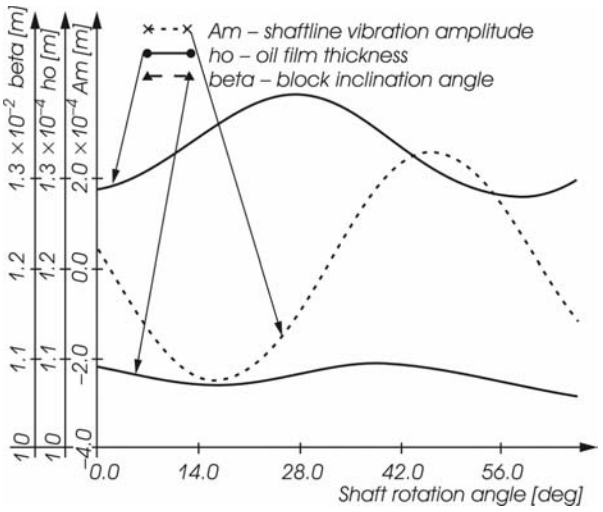

Fig. 9. The bearing operation parameters at 87 r.p.m.

Table 3. Stiffness and damping characteristics of the thrust bearing

ME speed (r.p.m.)	Oil film stiffness (N/m) × 10^9	Oil film damping (Ns/m) × 10^6	Thrust bearing global stiffness (N/m) × 10^9
40.0	4.49	0.61	2.06
51.2	1.64	1.41	1.14
60.0	12.4	1.14	2.91
72.0	19.5	1.45	3.18
87.0	31.4	1.90	3.39

only if the axial vibration amplitude is high. In this case, the strongly nonlinear property of the oil film becomes apparent (Fig. 8).

Computations for a typical thrust bearing were carried out using a bulk cargo ship. The parameters of the ship were as follows: carrying capacity 163 000 tons; length 283 m; main engine thrust bearing of the Sulzer type 6 RTA-76, with six pads with an outer diameter of 880 mm, an inner diameter of 445 mm, and a contact angle of 35.5°.

The axial vibration amplitudes of the power transmission system are the dynamic loads of the thrust bearing in the algorithm in question. It is necessary to know the preliminary values of the axial vibrations of the shaftline of the ship in order to determine the dynamic bearing characteristics. It should be noted that at an engine speed of 51.2 r.p.m. a torsional resonance takes place, and consequently, a high level of longitudinal vibration occurs due to the torsional–longitudinal coupling existing in the system. Consequently, the maximum dynamic load of the bearing occurs.

The operational parameters of the bearings at an engine speed of 51.2 r.p.m. (torsional resonance) are shown in Fig. 8, and those at a nominal engine speed of 87 r.p.m. are shown in Fig. 9. At this speed, the sixth longitudinal harmonic of the power transmission system is dominant. The thrust-bearing characteristics at a nominal engine speed (Fig. 9) can be treated as linear, i.e., harmonic excitation (an axial vibration amplitude) causes a harmonic response (operational parameters: the thickness of the oil film and the angle of inclination of the bleck). The dynamic characteristics of the thrust bearing analyzed are highly nonlinear at the engines torsional resonance speed (Fig. 8). A scarcity of lube oil film occurs at a shaft rotation angle of about 10°–40°. The thrust bearing cannot work continuously in these conditions.

The stiffness of the oil film and the damping, as well as the global stiffness of the thrust bearing analyzed, are given in Table 3. The stiffness of the thrust-bearing steel construction with its foundation in the double bottom is estimated as 3.8×10^9 N/m.

The engine's maker recommends a total stiffness for the thrust bearing equal to 3.2×10^9 N/m, which is constant and independent of the rotational speed and the loading. The axial vibrations of the free end of the

crankshaft (normalized by the producers) are determined by the stiffness of the crankshaft and the cylindrical gas and mass forces. Therefore, the assumptions proposed by the main engine producers usually lead to a correct estimation of the axial vibrations. However, in some cases, the calculations might not be insufficiently accurate. The stiffness of the thrust bearing depends on the value of the static thrust and the dynamic load (the axial vibration amplitude), as well as on the main engine type and the ship's hull construction. The stiffness of the oil film is usually much higher than the steel construction, and therefore the changeability of the global (resultant) stiffness of the thrust bearing is weak. However, a sudden drop in the stiffness and a damping increase in the revolution of the torsional vibration can be observed.

4.3 Axial dampers

Axial dampers are applied in all low-speed marine engines to mitigate the axial vibration amplitudes of the free end of the crankshaft. Apart from the mitigation of the vibration amplitudes, an axial damper introduces an additional excitation source for the ship's hull and the vibrations of the superstructure.

Generally, the operating principles of dampers are all the same. A crankshaft flange located on the free end has the highest axial vibration amplitudes. The vibrating flange pumps over the lube oil between two chambers located on both sides of the flange. The flow of the lube oil can be controlled by a change in the cross-sectional area of the special oilways. The main engine producers proposed mathematical models of the axial damper. The old models of the dampers are limited to a single, linear spring (between the crankshaft and the engine frame) with constant characteristics. Nowadays, a typical model of a damper is as follows: its mass is connected to the crankshaft by a spring (very soft) and damping elements, and to the engine frame by another spring element. In the mass models, the equivalent part of the damper houses the supports. All the elements are still linear and constant, and are independent of the engine speed and damper loading.

Specialized software for analyzing the stiffness and damping characteristics of the lube oil film on the axial damper has been developed. The Reynolds equation, which describes the pressure distribution in an oil film, is analogical to the expression used in the thrust-bearing algorithm. Energy losses due to the drag of the lubricating oil flow between the damper chambers are taken into account in the second part of the calculation algorithm. The values of the drag coefficients are assumed according to Streeter.[10]

The mutual interaction of the axial vibrations of the tanker ship (of 90000 dwt and 246.9 m length) and the

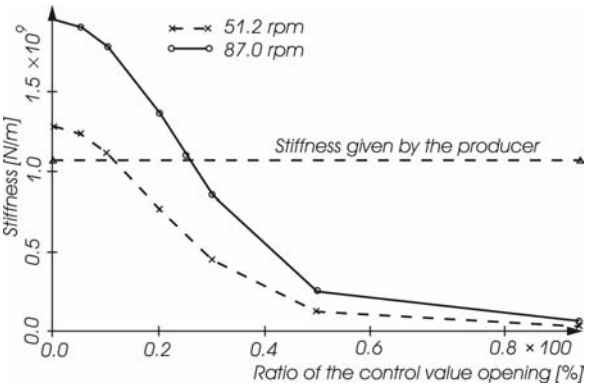

Fig. 10. Damper stiffnesses at different control valve opening ratios

damper performance parameters was taken into account. The axial damper of the main engine of the Sulzer 6 RTA-76 type (as described in Sect. 4.2) has a flange of outer diameter 400 mm and inner diameter 150 mm. In the analysis, the values of the axial vibrations of the crankshaft must be known. Different ratios for the opening of a control valve were analyzed. The calculated results at the torsional resonance speed of the power transmission system as well as at the nominal speed of the engine are shown in Fig. 10. It should be stressed that the damper could be tuned to the stiffness of the producer, but for one engine speed only. If the opening ratio of the control valve is adjusted to 25%, then at the nominal engine speed, the calculated stiffness is equal to the one given by the producer, but at 51.2 r.p.m. the damper stiffness is almost half that value.

From now on, 25% of the opening ratio of the damper control valve has been assumed in the analysis. An analysis of the damper performance in relation to the axial vibration calculations was carried out over the full range of engine speeds. The damping characteristics of the damper as well as the minimal and maximal reactions acting on the engine body construction are shown in Fig. 11.

The axial damper effectively mitigates the vibration amplitudes of the free end of the crankshaft, but it is relatively ineffective at decreasing the axial vibrations at the shaft line. The total value of the external excitations (at the damper and thrust bearings) will not always be reduced after the application of a damper.

5 Calculations—measurement comparison

The methods described in Sects. 1–4 were verified by measurements performed on several types of ship.[11] The measuring methods are simple: spring contact indicators or touch-less, inductive or laser indicators are used.

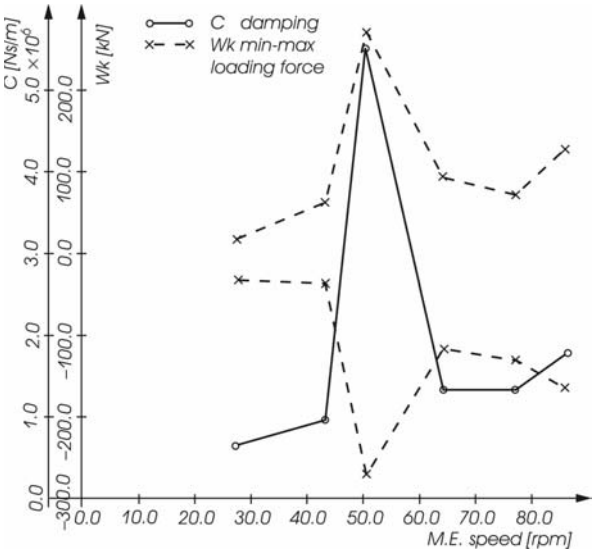

Fig. 11. Damping characteristics of the damper and reactions at 25% opening ratio

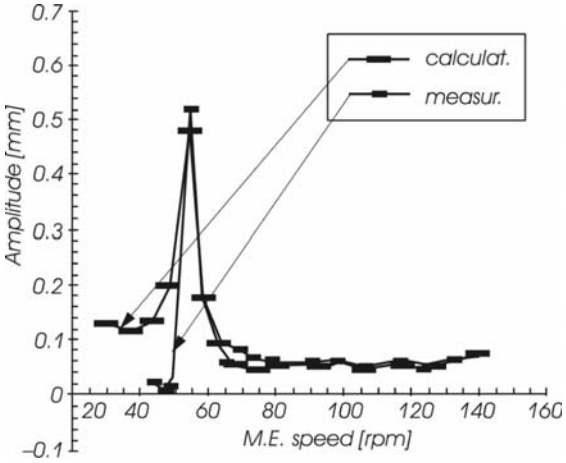

Fig. 12. 7th harmonic longitudinal vibrations

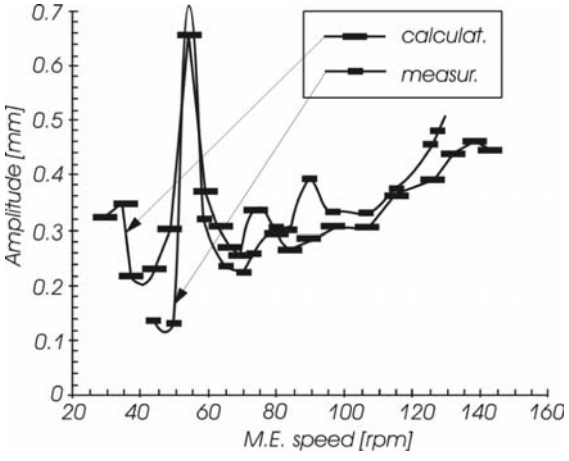

Fig. 13. Total longitudinal vibrations

The propulsion systems analyzed are equipped with axial dampers. The verification example was based on the container ship 1100 TEU (length 159 m; breadth 24 m; draught 8.5 m). The main engine, MAN B&W type 7 S50MC, was mounted, and its parameters were 10 010 kW and 127 r.p.m. The four-blade propeller had a diameter of 5.7 m and a mass of 18 100 kg. The torsional vibration resonance is laid around a main engine speed of 54 r.p.m. The calculations—measured comparisons of the total and the 7th harmonic longitudinal vibrations of the free end of the crankshaft are shown in Figs. 12 and 13.

The calculated crankshaft vibration amplitudes correlated well with the measured vibrations both at the rated speed and where torsional vibration resonance appeared. The experimental verification of the ships analyzed confirmed that the assumptions about the mathematical models of the marine power transmission systems and their boundary conditions were correct.

6 Propeller—crankshaft phasing

There are two main sources of dynamic excitations of marine power transmission systems: the hydrodynamics induced by a propeller, and the gas and mass cylindrical forces. The phase of the hydrodynamic forces depends on the position of the propeller blades. The phase of the cylindrical forces depends on the position of the cranks. The relative phase of these two types of force has a large influence on the vector sum of the excitation if the forces are of the same order of magnitude. Propulsion systems with the same number of cylinders as of propeller blades are the most dangerous because they have the same main harmonic excitation order. Nowadays, designers avoid these types of propulsion system. Sometimes, this dangerous phenomenon can be observed in other types of propulsion system. For example, for an eight-cylinder engine, the fifth harmonic component of the cylindrical forces is relatively high. A propulsion system with an eight-cylinder main engine and five-blade propellers may have unexpectedly high excitations. After changing the phase, the excitations should almost disappear.

The excitation from the engine to the hull is transmitted through the thrust bearing and the axial vibration damper. In my opinion, it is most important to minimize the dynamic reaction of the thrust bearing. The object is to reduce the thrust variations from the engine to the ship at a nominal or exploitation speed. The phase of the engine torque depends on the engine type, the mean

pressure indicated, and the order number. The phase of the propeller thrust from the wake field depends on the propeller and design of the hull shape. Separate calculations are necessary for each individual plant to determine the phases.

An example is presented of the optimization of the thrust-bearing longitudinal dynamic reaction. The analysis was performed for a 4400 TEU container carrier equipped with a Sulzer 8 RTA 96C-type engine. The parameters of the propulsion system were as follows: eight-cylinder engine, power, 44 000 kW; speed, 100 r.p.m; five-blade propeller, diameter, 8.4 m; mass, 74 000 kg.

Two sources for the thrust-bearing reactions are taken into account: reactions coming from coupled axial vibrations, and those coming from hydrodynamic forces induced on the propeller. The dynamic thrust coming from the propeller is the result of the uncoupled axial vibration calculations. Coupled, torsional–bending–axial vibration calculations lead to the determination of the dynamics arising from the main engine.

The first two propeller-blade harmonic components (the 5th and the 10th) are taken into account. The frequencies of the higher components are significantly higher than the natural frequencies of the ship's main structures and have no practical importance. The ship's loading conditions have a strong influence on the hydrodynamic forces. Therefore, full loading and ballast conditions were taken into account. The exploitation range of the engine speed was analyzed. The 5th harmonic components of the thrust-bearing reactions coming from the propeller and from the main engine are shown in Fig. 14.

The order of magnitude of the thrust-bearing reactions coming from different sources is the same for both harmonic components. For the engine speeds, the main engine forces compensate for the hydrodynamic forces on the thrust bearing. This phenomenon can be observed for both of the ship's loading conditions. Therefore, for the propulsion system analyzed, i.e., propeller—crankshaft phasing, is legitimate. The summary excitations of the ship's hull can be minimized. The dynamic behavior of the ship's hull and superstructure can be significantly improved at relatively little low cost.

Figure 15 shows the optimal phase angle for both the harmonic components and the ship's loading conditions. The optimal phase angle of the propeller relative to the crankshaft was determined with the assumption that for the given main engine speed, the total thrust bearing reaction should be minimal, i.e., the difference between the phase angles is equal to 180°. It is clear that the phase angle does not change while the main engine is running. For a given propulsion system, only one phase angle can be assumed.

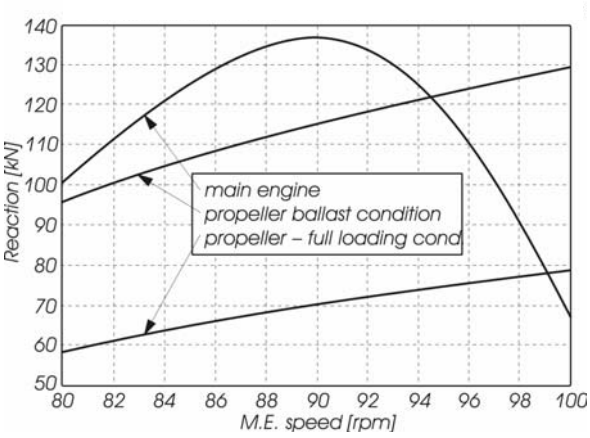

Fig. 14. The 5th harmonic components of the thrust-bearing reactions

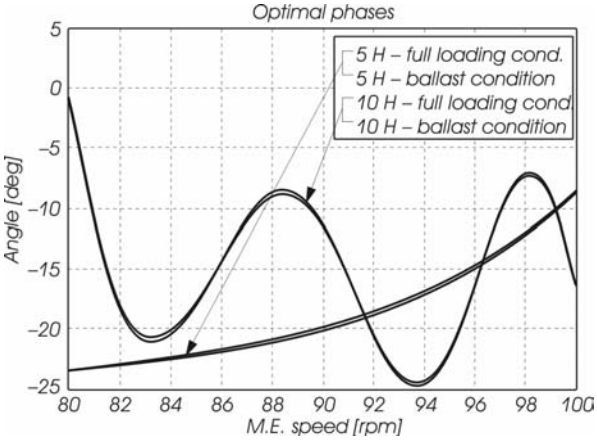

Fig. 15. Relative, optimal phase angle of the propeller and the crankshaft

For the propulsion system analyzed, the optimal phase angle changes depending on the main engine speed function and the ship's loading condition. Only one phasing can be chosen. The magnitude of the 10th harmonic component of the thrust-bearing reaction is much smaller than that of the 5th harmonic component. What is more, the frequency range of the 10th harmonic is considerably higher than the natural frequencies of the deckhouse and the rest of the ship's main structures. Therefore, for further analyses, only the 5th harmonic component has been analyzed.

Separate calculations for the ship's hull and deckhouse vibrations show that near a main engine speed of 90 r.p.m., deckhouse resonance vibrations with the 5th harmonic excitation can appear (the first vertical–longitudinal natural frequency of the superstructure is equal to ~7.5 Hz). If minimal excitations for this engine speed are demanded, then the propeller blade has to be rotated at an angle of –20.5° (contrary to the for-

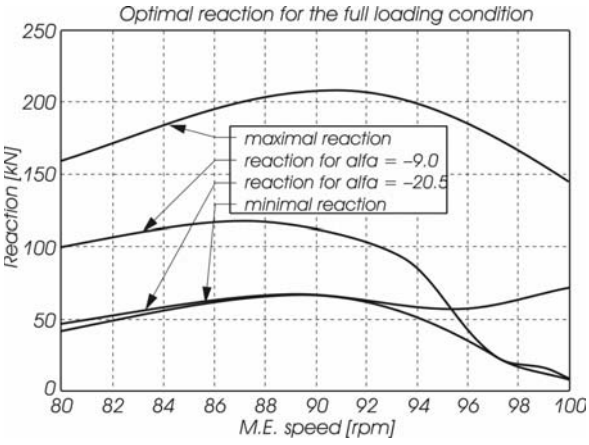

Fig. 16. The thrust bearing reactions for the ship's full loading condition

ward revolution of the propulsion) in relation to the first crank of the crankshaft. Therefore, the propeller blade should be delayed in relation to the first cylinder piston.

On the other hand, the most important thing is the vibration level in the engine at nominal speed. The superstructure vibration speeds are contracted and normalized at the nominal speed, which is equal to 100 r.p.m. The optimal phase angle of the propeller is equal to –9.0° for this engine speed.

Both phase angles (–9.0° and –20.5°) will be analyzed in further calculations. Figure 16 shows levels of the thrust-bearing reactions for the ship's full loading condition. These include the following reaction (deckhouse excitations) cases: the maximal reaction (an algebraic sum of the reactions from the propeller and the engine, i.e., the worst case); the minimal reaction (the algebraic difference of the reactions, i.e., the best possible case); and the reaction level when phase angles of –9.0° and –20.5° are applied.

The quotient for the best and the worst thrust bearing dynamic reactions is very high, and can be ten times higher than the minimum. The biggest difference is expected near the deckhouse resonance revolutions area, i.e., ~90 r.p.m. This numerical analysis, which was verified by measurements, was performed for a real ship. Unacceptable vibration speeds in the container deckhouse were lowered six-fold after the propeller was phased properly. Therefore, this type of analysis should be performed as standard because of its relatively low cost and huge beneficial effect.

7 Conclusion

On the basis of the analysis presented above, it may be assumed that a marine power transmission system can be analysed as an isolated system away from the ship's hull providing that the determination of the boundary conditions and the coupling coefficients is very good. The experimental verification with several ships confirmed that the mathematical model of the propulsion system presented and its boundary conditions is correct. The crankshaft—shaftline system should be considered as a linear mechanical system with nonlinear boundary conditions. The stiffness and damping characteristics of the damper and the thrust bearing should be determined for several engine speeds. Feedback between the boundary conditions and the level of axial vibrations should be taken into account in the analysis method.

All types of coupling should also be taken into account, otherwise the analysis, which takes only uncoupled axial vibrations of marine propulsion systems into account, might contain a serious error. The correct estimation of the foundation stiffness characteristics of the crankshaft has a significant influence on the stiffnesses and coupling coefficients of the crankshaft. The propulsion system's axial vibrations are more dangerous if the foundation flexibility of the crankshaft is increased (except in the torsional vibration resonance region). In my opinion, propeller—crankshaft phasing should be strongly recommended.

References

1. Jakobsen SB (1991) Coupled axial and torsional vibration calculations on a long-stroke diesel engine. Soc Nav Archit Mar Eng 99:405–419
2. Camisetti C, Molinari R (1982) Vertical and axial vibration of a ship propulsion system. Quaderno 49:16–28
3. Jenzer J (1987) Vibration analysis for modern ship machinery. Sulzer, Winterthur
4. Reed FE, Bassett N (1989) Further studies of propeller-excited vibrations on a Great Lakes cargo ship. SNAME Trans 97:375–396
5. Jenzer J, Welte Y (1991) Coupling effect between torsional and axial vibrations in installations with two-stroke diesel engines. Wartsila NSD
6. Viner AC (1971) Ship vibration. Lloyds Register of Shipping, No. 53, pp 2–46
7. Dien R, Schwanecke H (1973) Die propellerbedingte wechselwirkung zwischen schiff und maschine. Teil 2. Motortechnische 34(11)
8. Murawski L (2001) Influence of journal bearing modeling method on shaft line alignment and whirling vibrations. PRADS, 8th International Symposium on Practical Design of Ships and Other Floating Structures, Elsevier, pp 1205–1212
9. Barwell FT (1979) Bearing systems. principles and practice. Oxford University Press, Oxford
10. Streeter E (1961) Handbook of fluid dynamics. McGraw-Hill, New York
11. Murawski L (2001) Axial vibrations of a marine shaft line: calculations and measurements comparison. 4th International Conference on Marine Technology, Wessex Institute of Technology, UK, WIT, pp 299–308